Identification of three unexpected new psychoactive substances at an Australian drug checking service

Jess L. Algar,[a,b] Douglas J. Lawes,[a] Adam J. Carroll,[a] David Caldicott,[c,d] and Malcolm D. McLeod[a]*

[a] Research School of Chemistry, Australian National University, Canberra, Australian Capital Territory, Australia
[b] CanTEST Health and Drug Checking Service, 1 Moore Street, Canberra, Australian Capital Territory, Australia
[c] Emergency Department, Calvary Public Hospital, Canberra, Australian Capital Territory, Australia
[d] ANU Medical School, Australian National University, Canberra, Australian Capital Territory, Australia

* Corresponding author: malcolm.mcleod@anu.edu.au; +612 6125 3504

Abstract

Drug checking is a harm reduction measure which provides people with the opportunity to confirm the identity and purity of substances before consumption. The CanTEST Health and Drug Checking Service is Australia's first fixed-site drug checking service, where clients can learn about the contents of the samples they provide whilst receiving tailored harm reduction and health advice. Three samples were recently presented to the service with the expectation of 4-fluoromethylphenidate (4F-MPH) **1**, methoxetamine (MXE) **2** and 3-methylmethcathinone (3-MMC) **3**. The identity of all three samples did not meet these expectations and remained unknown on-site as no high confidence identifications were obtained. However, further analysis by nuclear magnetic resonance (NMR) spectroscopy, high resolution gas chromatography-electron ionisation-mass spectrometry (GC-EI-MS) and liquid chromatography-electrospray ionization-mass spectrometry (LC-ESI-MS) at the Australian National University (ANU) allowed for the structure elucidation of the three samples as 4-fluoro-α-pyrrolidinoisohexanophenone (4F-α-PiHP) **4**, 1-(4-fluorobenzyl)-4-methylpiperazine (4F-MBZP) **5** and *N*-propyl-1,2-diphenylethylamine (propylphenidine) **6** respectively. Given all three samples were not of the expected identity and have not yet been described in the literature, this study presents a full characterisation of each substance. As exemplified by this rapid identification of three unexpected new psychoactive substances, drug checking can be used as an effective method to monitor the unregulated drug market.

Keywords

Drug checking, pill testing, harm reduction, drugs, new psychoactive substances

1. Introduction

'Drug checking', also known as 'pill testing' in Australia, is a harm reduction intervention that allows people who use drugs to test the content and purity of their substances prior to consumption.[1-4] Drug checking can provide information on the presence and quantity of expected active ingredients, as well as the presence of potentially harmful adulterants, or substitutions. By providing timely and accurate information on drug contents, drug checking can empower people who use drugs to make informed decisions about their substance use, reduce their risk of overdose and other adverse effects, and provide access to harm reduction and treatment services. Drug checking can also effectively monitor the unregulated drug market and guide public health responses to it by generating data on drug trends, or availability and harms at the level of the consumer.[5,6]

Drug checking is a promising intervention to address the emerging challenges posed by new psychoactive substances (NPS) in the global drug market.[7,8] They comprise of a diverse group of synthetic drugs that mimic the effects of established illicit drugs, such as heroin, ketamine, LSD and MDMA. Constantly evolving to evade legal control and detection, NPS pose challenges for drug surveillance, regulation and public health responses.

The CanTEST Health and Drug Checking Service pilot was launched by the ACT Government in July 2022, as Australia's first fixed-site drug checking service.[9,10] The service is operated by Directions Health Services, with the assistance of the Canberra Alliance for Harm Minimisation and Advocacy and Pill Testing Australia. CanTEST aims to reduce the harms associated with drug use by providing free and confidential chemical analysis of drugs, as well as tailored harm reduction advice and counselling to service users. The service is available to members of the public in possession of drugs intended for personal use. Service users are also offered information on how to reduce their risk of overdose and other adverse effects, how to access treatment services, and how to dispose of unwanted drugs safely. The CanTEST Health and Drug Checking Service is a pioneering initiative with the capacity to rapidly address the challenges posed by NPS in the Australian drug market.[11]

In June 2023 three samples were presented to the CanTEST service for analysis. In each case, analysis at the service returned results inconsistent with client expectation. Subsequent laboratory analysis of these substances identified each as consisting of primarily one compound, for which little information was available in the scientific literature. Herein we report the chemical structures and analytical data for three potential stimulant and entactogen

NPS presented at the service: 4-fluoro-α-pyrrolidinoisohexanophenone (4F-α-PiHP) **4**, 1-(4-fluorobenzyl)-4-methylpiperazine (4F-MBZP) **5**, and *N*-propyl-1,2-diphenylethylamine (propylphenidine) **6**.

2. Experimental

2.1. General

Solvents were laboratory reagent grade unless otherwise stated. The three reported compounds were presented to CanTEST as samples for drug checking against their expected identities. Structural elucidation of all three compounds was conducted by analysis of either the residue collected from the isopropyl swab used to clean the Fourier Transform Infra-Red (FTIR) spectrometer or the 1 mg/mL sample used for Ultra-Performance Liquid Chromatography-Photo-Diode Array (UPLC-PDA) analysis.

2.2. FTIR Analysis

Following cleaning and a background scan on a Bruker Alpha II FTIR instrument equipped with a diamond Attenuated Total Reflectance (ATR) stage and zinc selenide optics, approximately 1-2 mg of powder of each sample were loaded onto the instrument for analysis. The software used for the analysis was the 'OPUS Drug ID Wizard' (version 8.2.21) with the following libraries: SWGDRUG Infrared Library (version 2.1), TICTAC Drug Library (April 5, 2018), BCCSU FTIR-ATR Library of Tryptamines (February 22, 2023), BCCSU FTIR-ATR Library (February 22, 2023) and a custom in-house library of previously identified and well-characterised compounds derived from client samples.

2.3. UPLC-PDA Analysis

The UPLC-PDA analysis[12] was performed on an ACQUITY UPLC H-Class PLUS fitted with an ACQUITY UPLC Photodiode Array (PDA) Detector (210 to 400 nm at 20 points per second). The UPLC separation of compounds was performed using an ACQUITY UPLC CSH C_{18} column (50 × 2.1 mm, 1.7 µm) and a column temperature of 40 °C, eluting with a gradient consisting of the following mobile phases: 0.1% formic acid in water and methanol. A gradient elution program at a flow rate of 0.5 mL/min was applied, where the percentage of organic solvent was linearly changed: 0 min, 3%; 0.3 min, 3%; 3 min, 41.5%; 3.1 min, 70%; 3.6 min, 70%; 3.7 min, 3%; 6.2 min, 3%. The total analysis time was 6.2 min. The samples (0.1 mg/mL) were prepared in the initial chromatographic eluant, filtered (0.2 µm) and kept at 12 °C in the sample manager prior to injection (1 µL).

2.4. Nuclear Magnetic Resonance (NMR) Analysis

One and two dimensional ^{1}H and ^{13}C NMR spectra were acquired in chloroform-*d* ($CDCl_3$) at 298 K on a Bruker Avance III HD 800 spectrometer (800.13 MHz ^{1}H, 201.22 MHz ^{13}C) equipped with 5 mm TCI cryoprobe. Chemical shifts (δ) are reported in parts per million with ^{1}H shifts referenced to the residual solvent peak ($CHCl_3$: ^{1}H δ 7.26) and ^{13}C shifts referenced to either the solvent peak ($CDCl_3$: ^{13}C δ 77.16) or the residual solvent cross-peak ($CHCl_3$: ^{13}C δ 77.36) . Coupling constants (*J*) are reported in Hertz (Hz). Standard abbreviations indicating multiplicity were used as follows: m = multiplet, t = triplet, d = doublet, s = singlet.

2.5. Gas Chromatography-Electron Ionisation-Mass Spectrometry (GC-EI-MS) Analysis

To a scintillation vial containing the isopropyl alcohol swab used to clean the FTIR spectrometer for each of the three samples was added methanol (MeOH, 1 mL). Following thorough mixing, 100 µL of each of the three solutions were combined with 900 µL of MeOH to create an approximately 0.1 mg/mL sample which could then be directly analysed by gas chromatography–electron ionisation-mass spectrometry (GC-EI-MS). The GC-EI-MS analyses were undertaken on two different instruments: one with a low mass resolution single quadrupole mass selective detector (low-resolution GC-EI-MS) and one with a high resolution quadrupole time-of-flight (QToF) mass spectrometer (high-resolution GC-EI-MS). The low-resolution instrument consisted of an Agilent 7890 GC coupled to an Agilent 5975C Inert Mass Selective Detector while the high-resolution instrument consisted of an Agilent 8890 GC coupled to an Agilent 7250 QToF mass spectrometer. Both instruments were equipped with Gerstel MPS preparative autosamplers that performed sample injections and washed the injection syringe twice each with ethyl acetate and methanol before and after each injection. The GC method used was essentially the same on each system. The carrier gas was ultra-high purity helium. Sample injection volume was 1 µL. The split/splitless inlet was operated in split mode (split ratio 25:1) at a temperature of 250 °C with a septum purge flow of 3 mL and purge flow to the split vent of 20 mL/min at 1 min. The GC column was a 40 m long (including 10 m of film-free guard precolumn) VF-5ms 5% phenyl polydimethylsiloxane column with internal diameter of 250 µm and film thickness of 0.25 µm (Agilent Part No. CP9013). Carrier gas flow through the column was 1 mL/min in constant flow mode. Initial oven temperature was 50 °C. This was held for 1 min before being ramped to 325 °C at 25 °C min^{-1} and held at 325 °C for 7 min. The total run time was 19 min. The heated transfer line to the MS was kept at 300 °C. Mass spectrometer settings on the low-resolution 5975C MSD were as follows:

source temperature 230 °C; quad temperature 150 °C; solvent delay 5 min; EM setting mode gain with gain factor 1; normal scanning; trace ion detection off; low mass 40; high mass 600; threshold 0; A/D samples 2.

Mass spectrometer settings on the high-resolution 7250 QTOF were as follows: source temperature 200 °C; EI mode "standard"; emission fixed at 0.2 µA; electron energy 70 eV; solvent delay 5 min; quad cut-off mass 35 AMU; collision energy 0; TOF mass range 35 to 600 AMU; acquisition rate 5 spectra/sec; acquisition time 200 ms/spectrum; transients/spectrum 1940. A TOF mass calibration was carried out just prior to analysis, giving mass errors below 1 ppm.

To enable calculation of Kovats retention indices (RIs) for detected compounds, a mixture of six n-alkanes dissolved in anhydrous pyridine at a concentration of approximately 33 µg/mL each was analysed alongside the samples in separate runs of the same analytical batch. These n-alkanes were: C_{12}, C_{15}, C_{19}, C_{22}, C_{28} and C_{32}.

For low-resolution GC-EI-MS, data processing was performed using Automated Mass Spectral Deconvolution and Identification System (AMDIS) software (version 2.73) . To enable AMDIS to calculate RIs for detected components, the retention times of the six alkanes were determined by manual inspection of the data and entered into an AMDIS .CAL file. Raw data files were processed in AMDIS with the following settings: type of analysis 'use retention index data"; adjacent peak subtraction one; resolution = medium; sensitivity = medium; shape requirements low.

For high-resolution GC-EI-MS, data processing was performed using MS-DIAL software (Version 4.9.221218)[13] after conversion of the Agilent ".D" format raw data files to .abf format with Reifycs Analysis Base File Converter (2019 Version). Key MS-DIAL settings were as follows: minimum peak height 1000; accurate MS On; mass slice width 0.01 Da; mass accuracy for centroiding 0.0025; sigma window value 0.5; EI spectra cut off 10. The retention time / retention index information from the alkane mix RI calibration data were provided to MS-DIAL in its required text file format.

2.6. High Resolution Liquid Chromatography-Electrospray Ionisation-Mass Spectrometry (LC-ESI-MS) Analysis

The same samples created for the GC-EI-MS analysis were used for high mass resolution ultra-high performance liquid chromatography-electrospray ionisation-mass spectrometry

(LC-ESI-MS). This was conducted on a Dionex RSLC Nano liquid chromatograph (LC) coupled to a Thermo-Fisher Orbitrap Fusion ETD mass spectrometer via a Heated Electrospray Ionisation (H-ESI) ion source. Chromatographic separation was conducted using the loading pump of the LC flowing at 200 µL/min. The chromatographic column was a Waters Acquity Premier BEH C18 column (50 mm x 2.1 mm internal diameter, 1.7 µm particles), fitted with a VanGuard guard column (Waters Part No. 186009455). Mobile phase Solvent A was ultra-high purity water with 0.1% (v/v) LC/MS-grade formic acid (Thermo Scientific Product No. 85178) and Solvent B was LC/MS-grade acetonitrile (Fisher Chemical Optima LC/MS Product No. A955-4) with 0.1% (v/v) formic acid. The LC gradient program was started at 5% B, held for 2 min then increased linearly to 90% B between 2 and 10 min, held at 90% B until 12 min, decreased to 5% B between 12 and 12.1 min, then held at 5% B until 15 min. Total run time was 15 min. Injection volume was 5 µl. Column oven temperature was 40 °C. The mass spectrometer was operated in positive ion data-dependent MS/MS (ddMS2) mode. The H-ESI ion source settings were as follows: spray voltage static; positive ion voltage 3500 V; sheath gas 35; aux gas 7; sweep gas 0; ion transfer tube temperature 300 °C; vaporizer temperature 275 °C. The ddMS2 duty cycle, with cycle time set to 1 s, started with an MS1 survey scan in the Orbitrap (resolution 240,000; scan range 50-1000 *m/z*; RF lens % 60; polarity positive). Precursor ions identified by the survey scan were filtered by intensity with intensity threshold 1.0e5. Dynamic exclusion was set to exclude ions within 10 ppm of the selected ion for 6 seconds after 1 selection with exclude isotopes on. The data-dependent MS2 scan properties were as follows: isolation window 1.6 *m/z*; isolation offset off; activation type HCD; collision energy mode fixed; HCD collision energy 20, 30, 40 or 50%; detector type Orbitrap; Orbitrap resolution 30000; maximum injection time54 ms.

Visualisation and manual inspection of LC-ESI-MS data was performed in Thermo FreeStyle software (Version 1.7.73.12). Export of selected reference spectra to standard data exchange formats was performed using the MSConvertGUI tool (Version 3.0.21128-7376ae988) from the ProteoWizard software package.[14]

3. Results and Discussion

Three samples were presented to the CanTEST service during routine operation. The client reported the samples were supplied with ambiguous descriptions and were expected to be 4-fluoromethylphenidate (4F-MPH) **1**, methoxetamine (MXE) **2**, and 3-methylmethcathinone (3-

MMC) **3** (Figure 1). Analysis at the CanTEST service by FTIR and UPLC-PDA failed to identify the substances despite compounds **1**, **2** and **3** being present in the FTIR libraries used during the analysis. For all three samples a single peak of unknown identity was observed in the chromatogram produced by UPLC-PDA analysis, which indicated each to consist of one major compound. The swabs used to clean the FTIR ATR stage and the UPLC-PDA samples were therefore retained for further analysis at the Australian National University (ANU) detailed below.

Figure 1

3.1. Analysis of sample 1

The first sample was expected to be the stimulant drug 4F-MPH **1** (Figure 1). The FTIR analysis of this sample generated an absorption of 1678 cm^{-1} inconsistent with an ester and indicative of a conjugated carbonyl group,[15] a broad absorption between 2800-2200 cm^{-1} indicative of an amine salt[15] and C-H stretches at 2962 cm^{-1} and 2870 cm^{-1} (Figure S16). The LC-ESI-MS spectrum (Figure 2) revealed an ion (*m/z* 264.1758), suggesting the molecular formula for the proton adduct was $C_{16}H_{22}NOF$ (*m/z* 264.1764).

In the ^{1}H NMR spectrum (Figure S1), two doublet of doublet peaks were observed in the aromatic region at δ 8.04 and δ 7.24 (H_b and H_a respectively), characteristic of a *para*-substituted fluorinated aromatic ring. After identifying the attached carbons in the ^{1}H-^{13}C HSQC spectrum (Figure S3) it was evident that these ^{13}C peaks in the $^{13}C\{^{1}H\}$ NMR spectrum (Figure S2) were split into doublets, which further indicated the presence of a coupled ^{19}F atom. The ^{1}H-^{13}C HMBC spectrum (Figure S4) revealed only one multiple-bond C-H correlation between the aromatic ring and the remainder of the compound, from H_b to a quaternary carbonyl carbon at δ 195.51, indicating the aromatic ring was directly bound to the carbonyl group. The ^{1}H COSY spectrum (Figure S5) showed couplings between alkyl protons of the compound, situated in two distinct spin systems and likely separated by a nitrogen atom, given that the downfield nature of several peaks (H_c, H_g, and $H_{g'}$) are consistent with amine-bound CH environments. The same three protons also shared couplings to a broad proton peak at δ 12.52 (which is likely NH^{+}), further indicating the two alkyl spin systems surround a protonated tertiary amine. Combining the ^{1}H COSY and ^{1}H-^{13}C HSQC correlations, one alkyl system was found to contain a methine group, labelled ***c,*** bound to a diastereotopic methylene group, ***d***, which was further connected to an isopropyl group (methine ***e*** and methyls ***f*** and ***f'***). Multiple bond correlations in the HMBC were consistent with this alkyl system being attached

to the carbonyl through methine ***c***. The HSQC and HMBC data also revealed that the remaining alkyl spin system contained four methylene groups, forming a four carbon chain ***g-h-h'-g'*** whose ends attached to the protonated amine, forming a pyrrolidine ring. From this analysis, the first compound was identified as 4F-α-PiHP **4** (4-fluoro-α-pyrrolidinoisohexanophenone, Figure 1).

The proposed LC-ESI-MS fragmentation pathway (Figure 2, S19) of the proton adduct involves the loss of the pyrrolidine ring and sequential loss of the acyl substituent to account for the major fragments, *m/z* 151.0551, 123.0237 and the base peak 109.0444, which corresponds to the *para*-fluorobenzyl cation derived from extensive rearrangement. Another pathway generates the fragment *m/z* 207.1053 arising from loss of an isobutyl radical from the proton adduct. Also observed were the fragments *m/z* 140.1431 and 84.0804 corresponding to an iminium ion formed by loss of the fluorinated aromatic and carbonyl moieties followed by subsequent fragmentation. The former fragment *m/z* 140.1431 was also observed as the base peak in the high-resolution GC-EI-MS spectrum (Kovats RI = 1684.7, Figure S22).

Figure 2

This new cathinone derivative, 4F-α-PiHP **4**, is closely related to its non-fluorinated (α-PiHP)[16] and non-branched (4F-α-PHP) counterparts that have both been described in the scientific literature.[17] The reference material and GC-MS spectrum for 4F-α-PiHP **4** is available from Cayman Chemical but was not obtained as part of this study due to a projected 3-4 month delay for supply. *para*-Halogenated cathinones are well known and described as being capable of increasing the risks of serotonergic toxicity. *In vitro* studies suggest that they have the potential to be hepatotoxic by mitochondrial impairment.[18,19]

3.2. Analysis of sample 2

The second sample was expected to be MXE **2** (Figure 1), a dissociative drug with structural similarities to ketamine. The FTIR analysis of this sample revealed a broad absorption between 2800-1800 cm^{-1} indicative of an amine salt[15] and C-H stretches between 3000-2850 cm^{-1} (Figure S17). No absorption corresponding to a ketone was observed. The LC-ESI-MS spectrum (Figure 3) revealed an ion (*m/z* 209.1447), suggesting the molecular formula for the proton adduct was $C_{12}H_{17}N_2F$ (*m/z* 209.1449).

As with 4F-α-PiHP (**4**), two aromatic protons at δ 7.17 and δ 7.67 (H_a, H_b) were observed in the ^1H NMR spectrum (Figure S6) with similar ^1H and ^{13}C splitting patterns and ^1H COSY

couplings (Figures S7 to S10), indicative of the presence of a *para*-substituted fluorinated aromatic ring. However, in this case, multiple bond correlations from the ^{1}H-^{13}C HMBC spectrum (Figure S9) indicated the aromatic ring was directly bonded to a methylene group (labelled ***c***). From the ^{1}H-^{13}C HSQC spectrum (Figure S8), two diastereotopic methylene environments were identified (***d***, ***e***), with each integrating to four protons, which indicated the presence of a symmetrical moiety. The ^{1}H and ^{13}C shifts of methylenes ***d*** and ***e*** were consistent with them being attached to amine nitrogens, and with the observation of COSY couplings between the methylene protons, it was determined that they comprised a piperazine ring. The two methylene environments of the piperazine ring were differentiated through analysis of the HMBC correlations to methylene ***c*** and methyl ***f***. Lastly, the relatively downfield alkyl proton environment of the methyl protons (H_f) and methylene protons (H_c) indicated their attachment to each nitrogen of the piperazine ring. This analysis identified the second compound as 4F-MBZP **5** (1-(4-fluorobenzyl)-4-methylpiperazine, Figure 1).

The proposed LC-ESI-MS fragmentation pathway (Figure 3, S20) of the proton adduct involves the loss of the *para*-fluorinated benzyl cation to give the base peak *m/z* 109.0444. Fragmentation of the same bond but with hydrogen transfer and placing the charge on the piperazine ring accounts for another major fragment *m/z* 99.0912. Also observed was a was a fragment corresponding to loss of HF arising from fragmentation to form an ion-molecule complex and subsequent S_NAr reaction at the fluorinated position.[20] The former fragment *m/z* 140.1431 was also observed as the base peak in GC-EI-MS (Kovats RI = 1574, Figure S23).

Figure 3

This new benzylpiperazine derivative 4F-MBZP **5** was first prepared and evaluated in a study of 5-HT_2 serotonin receptor modulation.[21] It is closely related to the non-fluorinated counterpart MBZP, a well-known stimulant.[22,23] More recently 4F-MBZP **5** has been used as a MS probe to study the fragmentation of benzylpiperazine derivatives.[20] Benzylpiperazines have been described for many years, including halogenated varieties such as TFMPP, and pFBP.[24] The halogenated piperazines have the strongest hepatotoxic effects *in vitro*,[25] raising concerns of potential harms that might be associated with this product.

3.3. Analysis of sample 3

The third compound was expected to be 3-MMC **3** (Figure 1), a cathinone closely related to mephedrone (4-MMC). The FTIR analysis of this sample revealed a weak, broad absorption at 3306 cm^{-1} indicative of an aliphatic primary amine as well as a broad absorption pattern

between 3000-2400 cm^{-1} indicative of both an amine salt[15] and partially obscured C-H stretches (Figure S18). No absorption corresponding to an unsaturated ketone was observed. The LC-ESI-MS spectrum (Figure 4) gave an ion (*m/z* 240.1749), suggesting the molecular formula for the proton adduct was $C_{17}H_{21}N$ (*m/z* 240.1752).

Overlapping peaks in the aromatic region of the ^{1}H NMR spectrum (Figure S11) were resolved by the ^{1}H-^{13}C HSQC spectrum (Figure S13), which indicated the presence of two mono-substituted aromatic rings. Using ^{1}H COSY and ^{1}H-^{13}C HMBC spectra (Figures S15 and S14), multiple-bond correlations were followed within the aromatic environments and neighbouring alkyl groups, which allowed for the full assignment of each aromatic ring and determination of their connectivity through a diastereotopic methylene group (***h***), and a methine group (***d***) directly bound to a nitrogen atom. The ^{1}H spectrum also displayed two broad peaks at δ 10.40 and δ 10.06, indicative of diastereotopic protons of a protonated secondary amine (NH_2^+). Furthermore, the COSY spectrum showed the NH_2^+ protons were coupled to protons in methylene ***c*** and methine ***d***, confirming the connectivity about the nitrogen. Lastly, the COSY spectrum also showed proton-proton couplings from methylene ***c*** to methylene ***b*** and then to methyl ***a***, forming the *N*-propyl moiety and completing the structure. Thus, the third compound was identified as propylphenidine **6** (*N*-propyl-1,2-diphenylethylamine, Figure 1).

Figure 4.

The proposed LC-ESI-MS fragmentation pathway (Figure 4, S21) of the proton adduct involves the loss of propylamine to give a benzylic cation *m/z* 181.1008 as the base peak. Further rearrangement and loss of methyl radical gives a fragment *m/z* 166.0776 corresponding to $[C_{13}H_{10}]^{\bullet+}$. The GC-EI-MS spectrum revealed a base peak with *m/z* 148.1122 following the loss of a neutral toluene fragment from **6** (Figure 4, S24). Further fragmentation involving the loss of the propyl chain accounts for the other major fragment ion *m/z* 106.0651 observed by GC-EI-MS (Kovats RI = 1853, Figure S24).

Propylphenidine **6** was first reported in the scientific literature in 1943[26] where it and a range of derivatives were investigated for bronchodilator and stimulant activities, with the chemical synthesis reported some years later.[27] It is structurally related to the lefetamine (Santenol) marketed as an analgesic and anti-inflammatory with opioid effects, and the potential for misuse.[28,29] More recently in 2008 the *N*-ethyl (NEDPA) and *N*-isopropyl (NPDPA) variants were identified following seizure by the German authorities,[30] with subsequent reports of these compounds also emerging in other jurisdictions.[31] NEDPA is also known as ephenidine and is

a diarylethylamine dissociative agent. When the UK banned arylcyclochexylamine agents in 2013, NEDPA was one of the products that replaced it. This is a group of drugs that has been associated with multiple deaths.[32]

4. Conclusion

Drug checking has traditionally been associated with the provision of harm reduction services, and amelioration of the potential hazard to consumers in what is an undeniably hazardous and heterogeneous market.[1-4] What has been less well appreciated is the utility of drug checking in identifying completely new entities that have never been characterized previously.[5,6] Such identifications can be accelerated by access to well-equipped facilities with access to complementary techniques such as NMR and high-resolution MS.

Drug checking is a collaborative process between consumers, and those conducting the service. As such, the identification of unknown substances may arise from community concerns about substance identity or effects - they are provided to a trusted service for analysis, by willing participants who understand that the service exists to keep them safe. Drug checking services are perhaps one of the *most* likely places where truly novel products are likely to first present, and are situated in an environment where appropriate prudent advice can be provided, even in scenarios where an agent might not yet be identified. In the same way that emerging infectious disease monitoring networks can gain valuable time in the early identification of strains of particularly virulent agents, drug checking can be the first opportunity to identify agents of potential and particular harm.

5. Acknowledgements

The CanTEST Health and Drug Checking Service is operated by Directions Health Services with funding from ACT Health and support from Pill Testing Australia and the Canberra Alliance for Harm Minimisation and Advocacy.

6. References

1. Giulini F, Keenan E, Killeen N, Ivers JH. A Systematized Review of Drug-checking and Related Considerations for Implementation as A Harm Reduction Intervention. *J Psychoactive Drugs.* 2023;55(1):85-93. https://doi.org/10.1080/02791072.2022.2028203.
2. Maghsoudi N, Tanguay J, Scarfone K, et al. Drug checking services for people who use drugs: a systematic review. *Addiction.* 2022;117(3):532-544. https://doi.org/10.1111/add.15734.
3. Morgan J, Jones A. Pill-testing as a harm reduction strategy: time to have the conversation. *Med J Aust.* 2019;211(10):447-448 e441. https://doi.org/10.5694/mja2.50385.

4. Groves A. 'Worth the test?' Pragmatism, pill testing and drug policy in Australia. *Harm Reduct J.* 2018;15(1):12. https://doi.org/10.1186/s12954-018-0216-z.
5. Gine CV, Vilamala MV, Measham F, et al. The utility of drug checking services as monitoring tools and more: A response to Pirona et al. *Int J Drug Policy.* 2017;45:46-47. https://doi.org/10.1016/j.drugpo.2017.05.018.
6. Brunt TM, Nagy C, Bucheli A, et al. Drug testing in Europe: monitoring results of the Trans European Drug Information (TEDI) project. *Drug Test Anal.* 2017;9(2):188-198. https://doi.org/10.1002/dta.1954.
7. Peacock A, Bruno R, Gisev N, et al. New psychoactive substances: challenges for drug surveillance, control, and public health responses. *Lancet.* 2019;394(10209):1668-1684. https://doi.org/10.1016/S0140-6736(19)32231-7.
8. Shafi A, Berry AJ, Sumnall H, Wood DM, Tracy DK. New psychoactive substances: a review and updates. *Ther Adv Psychopharmacol.* 2020;10:2045125320967197. https://doi.org/10.1177/2045125320967197.
9. CanTEST Health and Drug Checking Service. 2023; https://www.health.act.gov.au/about-our-health-system/population-health/pill-testing (accessed June 29, 2023).
10. Directions: CanTEST Health and Drug Checking Service. https://directionshealth.com/cantest/ (accessed June 29, 2023).
11. Caldicott D, McLeod M. An entirely new illicit drug has been discovered by Australian chemists. Here's how they did it. 2022; https://theconversation.com/an-entirely-new-illicit-drug-has-been-discovered-by-australian-chemists-heres-how-they-did-it-192855 (accessed July 24, 2023).
12. Gray M, Rohde A. Targeted Analysis of Drugs for Pill Testing Applications. 2021; https://www.waters.com/nextgen/au/en/library/application-notes/2021/targeted-analysis-of-drugs-for-pill-testing-applications.html (accessed July 4, 2023).
13. Lai Z, Tsugawa H, Wohlgemuth G, et al. Identifying metabolites by integrating metabolome databases with mass spectrometry cheminformatics. *Nat Methods.* 2018;15(1):53-56. https://doi.org/10.1038/nmeth.4512.
14. Chambers MC, Maclean B, Burke R, et al. A cross-platform toolkit for mass spectrometry and proteomics. *Nat Biotechnol.* 2012;30(10):918-920. https://doi.org/10.1038/nbt.2377.
15. Maheux CR, Copeland CR. Chemical analysis of two new designer drugs: buphedrone and pentedrone. *Drug Test Anal.* 2012;4(1):17-23. https://doi.org/10.1002/dta.385.
16. Critical review report: α-Pyrrolidinoisohexanophenone (α-PiHP). 2022; https://cdn.who.int/media/docs/default-source/controlled-substances/45th-ecdd/a-pihp-eh_sb_edit-1.pdf?sfvrsn=628a3f2f_1 (accessed July 14, 2023).
17. Liu C, Jia W, Li T, Hua Z, Qian Z. Identification and analytical characterization of nine synthetic cathinone derivatives N-ethylhexedrone, 4-Cl-pentedrone, 4-Cl-alpha-EAPP, propylone, N-ethylnorpentylone, 6-MeO-bk-MDMA, alpha-PiHP, 4-Cl-alpha-PHP, and 4-F-alpha-PHP. *Drug Test Anal.* 2017;9(8):1162-1171. https://doi.org/10.1002/dta.2136.
18. Luethi D, Walter M, Zhou X, Rudin D, Krahenbuhl S, Liechti ME. Para-Halogenation Affects Monoamine Transporter Inhibition Properties and Hepatocellular Toxicity of Amphetamines and Methcathinones. *Front Pharmacol.* 2019;10:438. https://doi.org/10.3389/fphar.2019.00438.
19. Zhou X, Bouitbir J, Liechti ME, Krahenbuhl S, Mancuso RV. Para-Halogenation of Amphetamine and Methcathinone Increases the Mitochondrial Toxicity in Undifferentiated and Differentiated SH-SY5Y Cells. *Int J Mol Sci.* 2020;21(8). https://doi.org/10.3390/ijms21082841.
20. Chai Y, Jiang K, Sun C, Pan Y. Gas-phase nucleophilic aromatic substitution between piperazine and halobenzyl cations: reactivity of the methylene arenium form of benzyl cations. *Chemistry.* 2011;17(39):10820-10824. https://doi.org/10.1002/chem.201101790.

21. Herndon JL, Ismaiel A, Ingher SP, Teitler M, Glennon RA. Ketanserin analogues: structure-affinity relationships for 5-HT2 and 5-HT1C serotonin receptor binding. *J Med Chem.* 1992;35(26):4903-4910. https://doi.org/10.1021/jm00104a017.
22. Kikura-Hanajiri R, Kawamura M, Uchiyama N, et al. [Analytical data of designated substances (Shitei-Yakubutsu) controlled by the Pharmaceutical Affairs Law in Japan, part I: GC-MS and LC-MS]. *Yakugaku Zasshi.* 2008;128(6):971-979. https://doi.org/10.1248/yakushi.128.971.
23. Zuba D, Byrska B. Prevalence and co-existence of active components of 'legal highs'. *Drug Test Anal.* 2013;5(6):420-429. https://doi.org/10.1002/dta.1365.
24. Welz A, Koba M. Piperazine derivatives as dangerous abused compounds. *Acta Pharm.* 2020;70(4):423-441. https://doi.org/10.2478/acph-2020-0035.
25. Dias-da-Silva D, Arbo MD, Valente MJ, Bastos ML, Carmo H. Hepatotoxicity of piperazine designer drugs: Comparison of different in vitro models. *Toxicol In Vitro.* 2015;29(5):987-996. https://doi.org/10.1016/j.tiv.2015.04.001.
26. Tainter ML, Luduena FP, Lackey RW, Neuru EN. Actions of a series of diphenyl-ethylamines. *Journal of Pharmacology and Experimental Therapeutics.* 1943;77(4):317-323.
27. Goodson LH, Wiegand CJ, Splitter JS. Analgesics; n-alkylated-1,2-diphenylethylamines prepared by the Leuckart reaction. *J Am Chem Soc.* 1946;68(11):2174. https://doi.org/10.1021/ja01215a018.
28. Mannelli P, Janiri L, De Marinis M, Tempesta E. Lefetamine: new abuse of an old drug--clinical evaluation of opioid activity. *Drug Alcohol Depend.* 1989;24(2):95-101. https://doi.org/10.1016/0376-8716(89)90071-9.
29. De Montis MG, Devoto P, Bucarelli A, Tagliamonte A. Opioid activity of lefetamine. *Pharmacol Res Commun.* 1985;17(5):471-478. https://doi.org/10.1016/0031-6989(85)90082-7.
30. Westphal F, Junge T, Jacobsen-Bauer A, Rösner P. Lefetamin-Derivate: alte Bekannte neu auf dem Drogenmarkt. *Toxichem Krimtech.* 2010;77:46-58.
31. Beharry S, Gibbons S. An overview of emerging and new psychoactive substances in the United Kingdom. *Forensic Sci Int.* 2016;267:25-34. https://doi.org/10.1016/j.forsciint.2016.08.013.
32. Wallach J, Kang H, Colestock T, et al. Pharmacological Investigations of the Dissociative 'Legal Highs' Diphenidine, Methoxphenidine and Analogues. *PLoS One.* 2016;11(6):e0157021. https://doi.org/10.1371/journal.pone.0157021.

Table 1. NMR data of compounds **4-6**

Structure	Label	Chemical Shifts (ppm)		Multiple bond correlations	
		^{1}H	^{13}C	^{1}H COSY cross-peaks	HMBC ^{1}H → ^{13}C cross-peaks
4 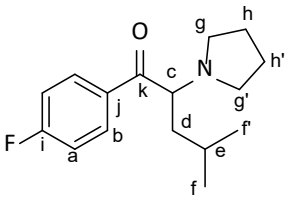	a	7.24	117.1	b	a', b, b', i, j
	b	8.04	131.6	a	a, a', b', i, k
	c	5.17	59.8	d, NH^+	d, e, g, k
	d	2.06, 1.90	39.9	c, e	c, e, f, f', k
	e	1.74	25.0	d, f	c, d, f, f'
	f	0.97	22.3	e	d, e, f'
	f'	0.98	23.1	e	d, e, f
	g	3.82, 3.63	48.6	g, h, NH^+	c, g', h, h'
	g'	3.83, 2.78	53.0	g', h', NH^+	c, g, h, h'
	h	2.18, 2.09	23.7	g, h	g, g', h'
	h'	2.21, 1.99	24.1	g', h'	g, g', h
	i		167.1		
	j		132.5		
	k		195.5		
	NH^+	12.52		c, g, g'	
5 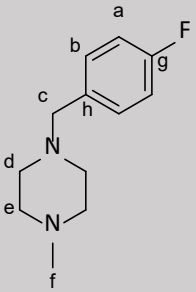	a	7.17	117.1	b	a', h, g
	b	7.67	133.6	a	b', c, g
	c	4.22	60.4		b, d, h
	d	3.95, 3.47	47.9	e	
	e	4.09, 3.49	49.8	d	
	f	2.91	43.1		e
	g		164.2		
	h		122.8		
	NH^+	13.8			
6 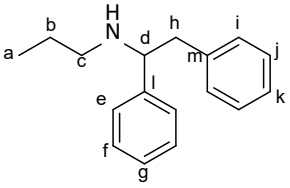	a	0.87	11.5	b	b, c
	b	1.98	19.6	a, c	a, c
	c	2.69	47.9	b, NH_2^+	a, b, d
	d	4.18	65.6	h	c, e, h, l
	e	7.45	128.8	f	d, f, g, l
	f	7.34	129.3	e	e, l
	g	7.33	129.4	f	e, f
	h	4.04, 3.48	40.9	d	d, i, l, m

	i	6.90	129.6	j	h, j, k, l
	j	7.10	128.5	k, i	i, m
	k	7.10	126.9	j	i, j
	l		133.8		
	m		135.8		
	NH_2^+	10.06, 10.40		c, d	

Table 2. High resolution LC-ESI-MS and GC-EI-MS data of compounds **4-6**

Compound	**$[M + H]^+$ formula**	**$[M + H]^+$ observed *m/z* (error, ppm)**	**LC-MS major fragment ions observed *m/z***	**GC-MS major fragment ions observed *m/z***
4	$[C_{16}H_{23}NOF]^+$	264.1758 (+0.0)	207.1053 151.0551 140.1431 123.0237 109.0444 84.0804	206.0964 140.1431 98.0961
5	$[C_{12}H_{18}N_2F]^+$	209.1447 (-1.0)	189.1384 109.0443 99.0912	136.0548 109.0444 44.0492
6	$[C_{17}H_{22}N]^+$	240.1749 (+0.8)	181.1008 166.0776	148.1122 106.0651

Figures

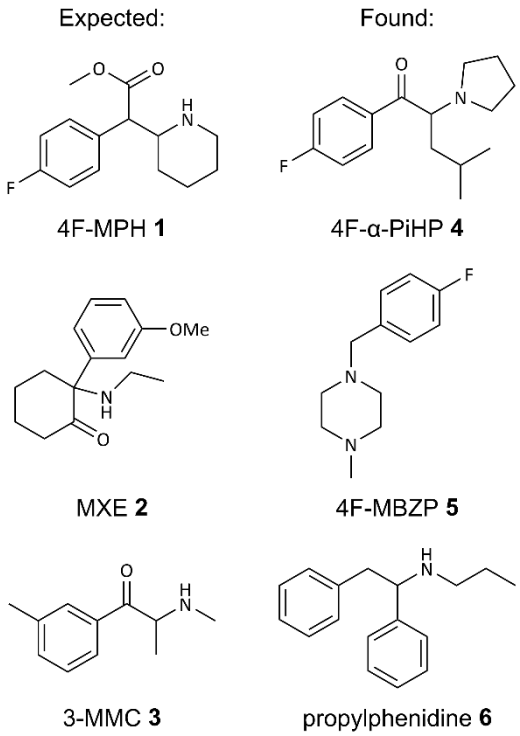

Figure 1. Expected and actual chemical structures of the three samples presented to the CanTEST Health and Drug Checking Service in June 2023.

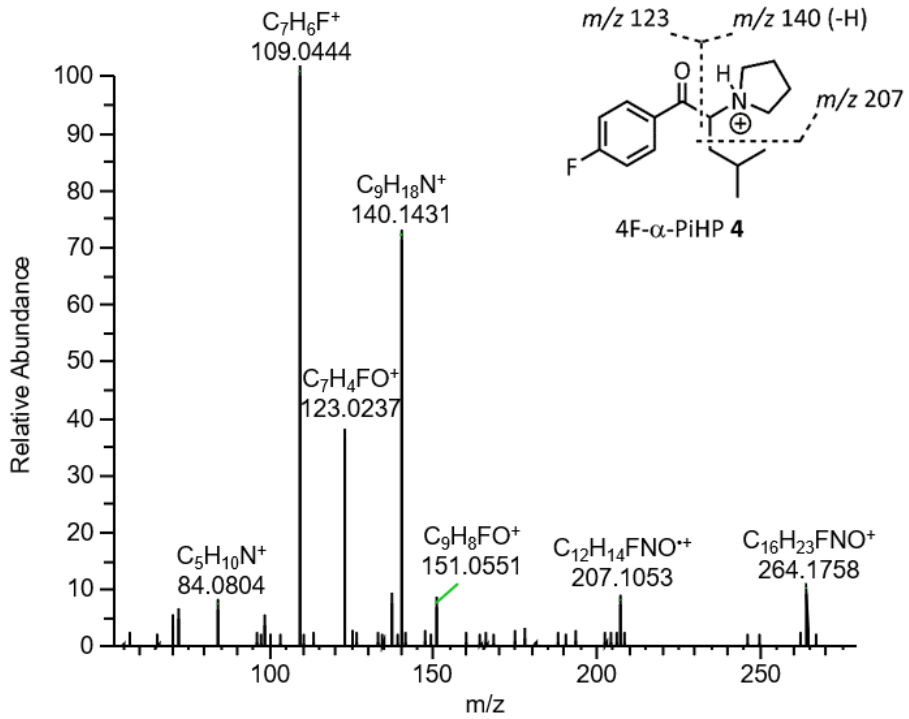

Figure 2. LC-ESI-MS product ion spectrum (NCE40) of the 4F-α-PiHP **4** proton adduct with selected bond fragmentation pathways shown. For further discussion of fragmentations see section 3.1 and Figure S19.

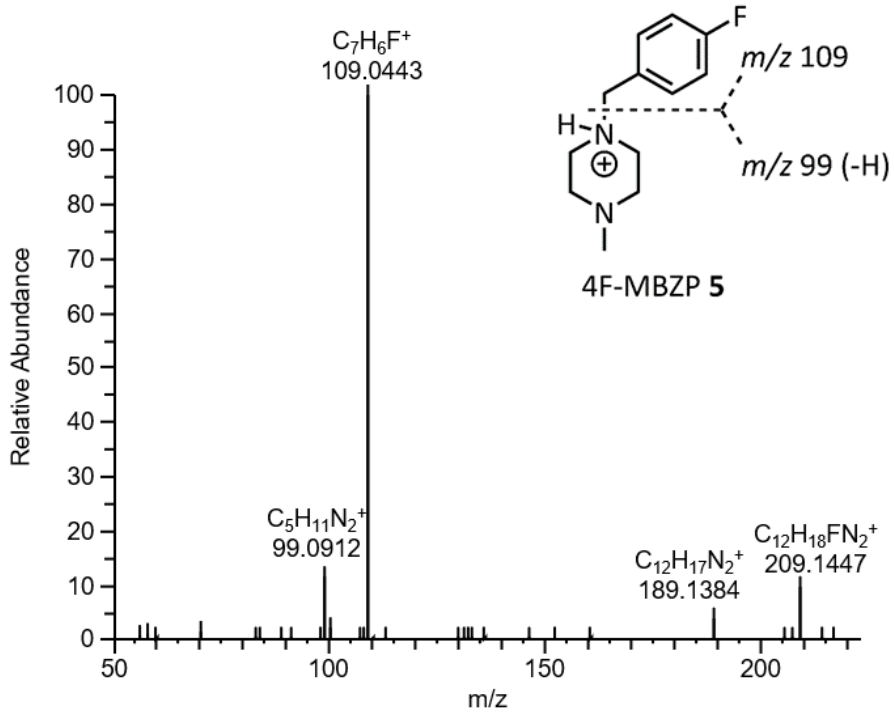

Figure 3. LC-ESI-MS product ion spectrum (NCE30) of the 4F-MBZP **5** proton adduct with selected bond fragmentation pathways shown. For further discussion of fragmentations see the section 3.2, ref. 20 and Figure S20.

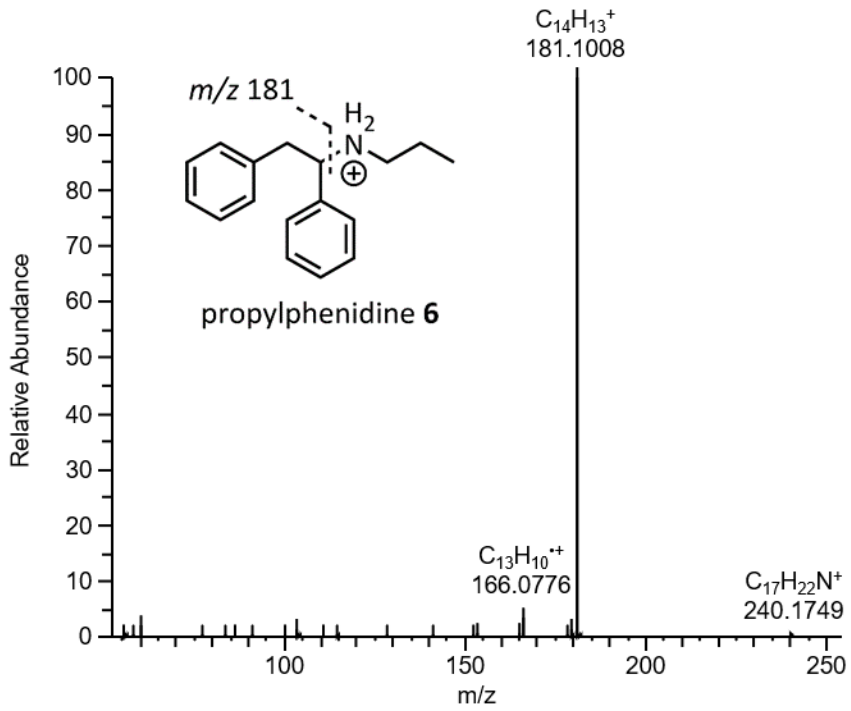

Figure 4. LC-ESI-MS product ion spectrum (NCE20) of the propylphenidine **6** proton adduct with selected bond fragmentations shown. For further discussion of fragmentations see the section 3.3 and Figure S21.